Geomechanics and Engineering, *Vol. 29, No. 3 (2022) 311-320*
https://doi.org/10.12989/gae.2022.29.3.311

Workability and compressive behavior of PVA-ECC with CNTs

Dongmin Lee[1a], Seong-Cheol Lee*[1] and Sung-Won Yoo[2b]

[1]*Department of Civil Engineering, Kyungpook National University, 80, Daehak-ro, Buk-gu, Daegu, 41566, South Korea*
[2]*Department of Civil and Environmental Engineering, Gachon University, 1342 Seongnamdaero, Sujeong-gu, Gyeonggi-do, 13120, South Korea*

(Received December 9, 2021, Revised March 5, 2022, Accepted March 11, 2022)

Abstract. TBM concrete segment requires a higher level of material properties compared to general concrete structures due to difficulties in maintenance and uncertainty in ground conditions. In this regard, recently, as one of the methods to achieve enhancement effect on concrete strength, many researchers have been focusing on adding CNTs to concrete mixture. However, even CNTs do not compensate the weakness that concrete exhibits brittle behavior after cracking. Separately, over the past few decades, a number of studies have been conducted on fiber reinforced concrete which exhibits ductile behavior due to fibers bridging cracks. However, only limited studies have been conducted to employ the advantages of the both materials together. In this study, an experimental program has been conducted to investigate the effect of CNTs on the workability and the compressive behavior of PVA-ECC which exhibits ductile tensile behavior with well-distributed cracks even without a conventional rebar. In addition to the compression test, SEM analysis has been also conducted for detailed investigation in the microstructure. The variable was the CNTs mix ratio, which were set to 0.00, 0.25, and 0.50 wt.% to the binding materials. It was observed though the test results that as the CNTs mix ratio increased, the workability considerably decreased with the reduced slump and slump flow. From the compression test results, it was also investigated that the compressive behavior was improved since the compressive strength, the strain corresponding to the compressive strength, and the modulus of elasticity increased with an increase of CNTs mix ratio. The contents of this paper will be useful for relevant research areas such as fiber reinforced concrete with CNTs which might be applied for high performance TMB concrete segments.

Keywords: cementitious composites; CNTs; compressive behavior; PVA fibers; SEM analysis

1. Introduction

As the development of technology makes the structure huge and ultra-high-rise, it is necessary to improve concrete performance such as strength and fluidity compared to conventional concrete. Underground structures are also required to secure performance. In the case of TBM tunnel segment, if the concrete quality is poor, construction might be delayed due to inrush of groundwater or soil due to cracks such as longitude and corner cracks during construction (Shi and Kong 2016, Xu *et al*. 2019); the TBM tunnel may collapse in the worst case. So, research is being actively conducted to prevent problems that may cause tunnel collapse (Chen *et al.* 2019, Xue *et al*. 2020). At the same time, it is necessary to conduct research on improving the performance of tunnel structures.

Recently, many studies investigated that the performance of concrete could be considerably improved by adding nanomaterials in concrete mixture. One of the frequently used nanomaterials in concrete is carbon nanotubes (CNTs), which were discovered by Iijima (1991). It was also investigated that CNTs had excellent electrical and thermal properties in addition to mechanical properties (Ruoff and Lorents 1995, Silvestro and Jean Paul Gleize 2020, Tanaka *et al.* 1994). Due to these advantages, research has been actively conducted in various fields such as geomechanics and structural engineering field (Camacho *et al.* 2014, Taha *et al.* 2018, Rousakis *et al.* 2014). However, if the weight ratio of CNTs is excessive or the dispersion of CNTs is poor, concrete performance is worse (Shao *et al.* 2017, Wang *et al.* 2019) and there is little or no improvement in ductility (Hawreen *et al.* 2018, Mohsen *et al.* 2019).

Meanwhile, even if CNTs are added in concrete mixture, the weakness of concrete exhibiting brittle behavior after cracking does not change. To attain ductile behavior after cracking in concrete, fibers have been being added in concrete mixture. In general, fiber reinforced concrete members can exhibits ductile behavior even after cracking, owning to fibers bridging cracks. In order to use fiber reinforced concrete as a structural member, lots of studies have been conducted; several researchers derived theoretical models to represent the tensile behavior of fiber reinforced concrete after cracking (Lim *et al*. 1987, Marti *et al*. 1999, Voo and Foster 2003, Lee *et al*. 2013b). Some researchers have focused on the cracking behavior (Deluce *et al*. 2014) or the tension stiffening behavior in the fiber reinforced concrete with conventional reinforcing bars (Bischoff 2003, Lee *et al*. 2010, Na and Kwak 2011, Lee *et al.* 2013a).

*Corresponding author, Associate Professor
E-mail: seonglee@knu.ac.kr
[a]Ph.D. Student
[b]Professor

ISSN: 2005-307X (Print), 2092-6219 (Online)

(a) Dry mix (b) Addition of water and CNTs (c) Addition of PVA fibers

Fig. 1 Mixing CNT dispersed aqueous solution and PVA fibers

Table 1 Mixing properties of PVA cementitious composites with CNTs

Specimen	CNT (wt. %)	Binder (kg/m^3)			Nonbinder (kg/m^3)				Water (kg/m^3)	W/B (%)	Fiber volume fraction (%)
		OPC	BFS	FA	Sand	Filler (CW)	Super plasticizer	SRA			
CNT-0.00	0.00	412	220	412	275	14	1.92	0.4	343	32.9	2.07
CNT-0.25	0.25	412	220	412	275	14	1.92	0.4	343	32.9	2.07
CNT-0.50	0.50	412	220	412	275	14	1.92	0.4	343	32.9	2.07

In order to effectively control cracks in TBM segments, several researches have been conducted to add fibers in concrete mixture (Caratelli *et al.* 2011, Gettu *et al.* 2004, Meda *et al.* 2019, Yan *et al.* 2013). Through the experimental tests results of these researches, it was investigated that fibers were effective to control cracks.

Among various fibers, polyvinyl alcohol (PVA) fibers are widely used since concrete with PVA fibers exhibits strain hardening behavior with multiple cracks even without conventional rebar (Kim *et al*. 2007; Shin *et al*. 2015). In addition to the structural behavior, it was also investigated that the resistance to chloride penetration and fire could be enhanced with PVA fibers (Magalhães *et al*. 2015; Wang *et al*. 2019).

In view of these points, it can be inferred that incorporating CNTs and PVA fibers is very useful for TBM tunnel segments which require high performance of concrete on mechanical properties as well as durability. However, the research about concrete with CNTs and PVA fibers together is very limited.

In this study, therefore, an experimental program is conducted to investigate the effect of CNTs on the workability and the compressive behavior of PVA engineering cementitious composites (PVA-ECC). The workability is evaluated through slump and slump flow measured during mixture while the compressive behavior is investigated through compression test with cylindrical specimens. For detailed investigation, the microstructure of PVA-ECC with CNTs is analyzed through SEM (Scanning Electron Microscope) images.

2. Materials

In order to investigate the effect of CNTs on the compressive behavior of PVA-ECC, an experimental program was conducted. The test variable was CNTs weight ratios in the mixture, which were varied from 0.0 to 0.5 wt.% since up to 0.5% of CNTs had been added in the literature (Collins *et al.* 2012, Li *et al.* 2005, Li *et al.* 2007, Musso *et al.* 2009, Yoo *et al.* 2018, You *et al.* 2017). For the mixture of PVA-ECC, this study adopted an ordinary mixture design broadly adopted in literature and industry in South Korea (Lee *et al.* 2019). The details about the materials are presented in the following sections.

Table 2 Properties of PVA fibers

Length (mm)	Diameter (mm)	Density (g/cm^3)	Tensile strength (MPa)	Young`s modulus (GPa)
12	0.039	1.3	1,600	25 ~ 40

2.1 PVA-ECC

Table. 1 shows the details of PVA-ECC mix proportion with CNTs. Total three CNTs mix ratios were considered, which varied from 0 to 0.5 wt.% by weight of binding materials. For the PVA cementitious composites (PVA-ECC), the mix proportion was adopted as presented in Table 1. In the mixture, ordinary Portland cement (OPC), blast-furnace slag (BFS) and fly-ash (FA) were used as binding materials. In many researches, BFS and FA have been added to materials as binder to improve concrete performance (Bera and Chakaborty 2015, Demirboğa 2003, Karabash and Firat 2015, Shooshpasha and Alijiani 2005, Yilmaz *et al.* 2017). The water/binder ratio (W/B) was fixed to 32.9%. Quartzite sand (grain size 0.1~1.7 mm) and hollow lightweight aggregate (CW) were used as fine aggregate while super plasticizer and shrinkage reducing admixture (SRA) were added to attain the performance for maintaining shape and workability. To attain ductile

Table 3 Summary of compressive test results on specimens

Specimen	Slump (cm)	Slump flow (cm)	Compressive strength (MPa)		Strain ($\times 10^{-3}$)		Modulus of elasticity (GPa)	
			Each	Average (S.D.)	Each	Average (S.D.)	Each	Average (S.D.)
CNT-0.00	23.0	55.5	32.6 37.5 35.6 34.2 34.5	34.9 (1.6)	3.14 4.10 3.82 3.71 4.14	3.78 (0.36)	12.5 12.8 12.8 12.1 12.2	12.5 (0.3)
CNT-0.25	13.0	29.0	39.6 37.1 37.8 39.2 38.1	38.4 (0.9)	4.15 3.35 4.22 3.72 3.81	3.85 (0.32)	12.9 13.8 12.7 13.4 13.4	13.3 (0.4)
CNT-0.50	0.00	20.0	47.9 45.1 45.7 45.4 46.4	46.1 (1.0)	4.14 4.49 3.97 4.51 4.58	4.34 (0.24)	14.0 13.9 14.9 13.6 14.2	14.1 (0.4)

behavior with well-distributed cracks, polyvinyl alcohol (PVA) fibers were added in the mixture. The fiber volumetric ratio was fixed to 2.07% as the manufacturing company provided. The properties of the PVA fibers were summarized in Table 2.

2.2 CNTs

CNTs are generally divided into two groups; single-walled carbon nanotubes (SWCNTs) and multi-walled carbon nanotubes (MWCNTs). Campillo *et al*. (2004) presented that MWCNTs had the compressive strength enhancement larger than SWCNTs. Chen *et al.* (2011) presented that MWCNTs being more affordable for industry application, and easier to disperse. In this study, therefore, multi-walled carbon nanotubes (MWCNTs) were used, which had a diameter of 10 nm and a length of 1.5 μm. In order to keep good dispersibility of CNTs, 3% aqueous solution with CNTs were prepared. 5% polycarboxylate superplasticizer (PCE) was added to the CNTs aqueous solution (Li 2005) and sonicated since CNTs are easy to be bounded by van der Waals` force and generally regarded as insoluble in water (Isfahani 2016).

3. Fabrication of specimens

It is already investigated that the workability and compressive behavior of PVA-ECC with CNTs are considerably affected by the mixing sequence. Park *et al*. (2021) experimentally investigated the effect of the mixing sequence on PVA-ECC with CNTs. In this study, based on the results of them, specimens of PVA-ECC with CNTs were fabricated according to the most optimal mixing sequence.

The detailed mixing sequence is as follows. At the first, cementitious composites were dry mixed, then water, CNTs, and PVA fiber were added and mixed in the order as shown in Fig. 1. After all the materials sufficiently mixed and dispersed, slump and slump flow were measured to investigate the effect of CNTs on workability. To investigate the compressive behavior of PVA-ECC with CNTs, five cylindrical specimens of 200 mm in height and 100 mm in diameter were fabricated for each mixture variable. The cylindrical specimens were cured for 28 days under the temperature of 20 ℃ and relative humidity of 70%.

On the age of 28 days, the compression test was conducted as shown in Fig. 2. Two strain gauges with 60 mm length were attached on the side faces of the specimens so that the compressive strain could be measured during the compression test. The compression was applied through Universal Testing Machine (UTM) with the loading rate of 0.2 mm/min.

In order for electron microscopy (SEM) analysis to investigate the effect of CNTs on the microstructure of PVA-ECC, several samples were taken around cracks after the compression test. A couple of scales were chosen for SEM analysis ranges; resolutions of x500 and x1000 were chosen to investigate the effect of CNTs along PVA fibers while resolutions of x1000 and x5000 were chosen to investigate dispersion of CNTs in cement paste.

4. Test results

4.1 Slump and slump flow results

The slump and slump flow measured after the mixing are presented in Table 3 and Fig. 3. As shown in the table and figure, when the CNTs mix ratio increased by 0.50 wt.%, the slump decreased by 100%, from 23 cm to 0 cm. Slump flow also significantly decreased by 36%, from 55.5 cm to 20.0 cm as well. This result indicated that as the CNTs mix ratio increased, both slump and slump flow considerably decreased. Especially, when 0.50 wt.% of CNTs was added in PVA-ECC mixture, there was little fluidity. This tendency is related to high surface area of CNTs which are better able to hold water molecules (Rhee 2013).

(a) Before (CNT-0.50)

(b) After (CNT-0.50)

Fig. 2 Compressive strength test setup

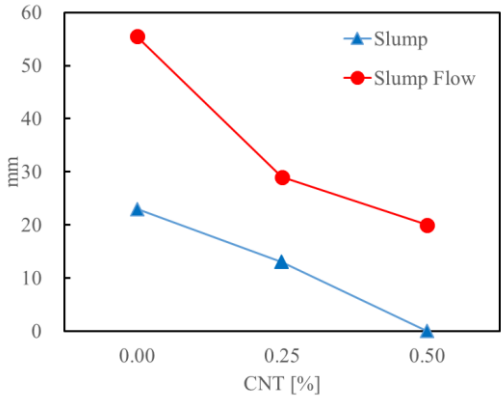

Fig. 3 Slump and slump flow

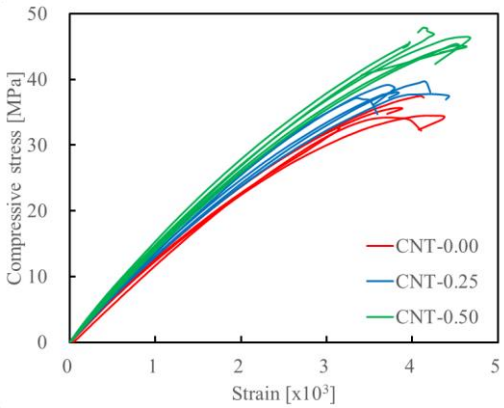

Fig. 4 Stress-strain curve of PVA-ECC with CNTs

Therefore, the workability should be considered to determine the appropriate CNTs mix ratio.

4.2 Compressive behavior

In order to investigate the effect of CNTs on the compressive behavior of PVA-ECC, the compression test was conducted at the age of 28 days. Fig. 4 shows the compressive stress-strain response measured through the test. It is noted that the post-peak behavior could not be measured due to the technical limitations of the test equipment. As can be seen in the figure, all the behaviors measured in the test exhibited similar tendency. Therefore, it can be seen that the reliability of the test results is high. Until the maximum compressive strength was reached, the convexity of the curve was observed to be different from that of ordinary concrete; the curvature of the compressive behavior curve was larger for ordinary concrete up to the compressive strength, whereas it was significantly smaller for PVA-ECC with CNTs. This is consistent with the test results of Shin *et al*. (2011), and it can be explained that PVA-ECC with CNTs does not contain coarse aggregates which are generally mixed in ordinary concrete.

Table 3 and Fig. 5 present the test results including the compressive strength, the strain corresponding to the compressive strength, and the modulus of elasticity that was evaluated in accordance with ASTM C469-02 (2002). Noted that the compression test results in the figures are the average of a total of five test results for each variable. As can be seen in the figure, the compressive behavior of PVA-ECC was considerably affected by CNTs. When the CNTs mix ratio was 0.00, 0.25, and 0.50 wt.%, the compressive strength was 34.9, 38.4, and 46.1 MPa. As the CNTs mix ratio increased by 0.50 wt.%, the compressive strength increased by 32.1%. For the strains upon the compressive strength were 3.78×10^{-3}, 3.85×10^{-3}, and 4.34×10^{-3}, respectively, and the modulus of elasticity were 12.5, 13.3, and 14.1 GPa, respectively, when the CNTs mix ratio was 0.00, 0.25, and 0.50 wt.%. As the CNTs mix ratio increased by 0.50 wt.%, both the strain upon the compressive strength and the modulus of elasticity increased by 14.8% and 12.8%, respectively. These test results are consistent with Nochaiya (2008) which presented that CNTs enhanced the compressive behavior of cement paste since CNTs reinforced the matrix composite phase. Therefore, it can be concluded that CNTs could enhance the compressive behavior of PVA-ECC as well.

In order to analyze the effect of CNTs on the shape of the compressive behavior curve, Fig. 6 shows the results of compressive behavior curve that the measured stress-strain responses have been normalized for the compressive strength and the corresponding strain. As compared in the figures, the shape of the compressive behavior curve was little affected by the CNTs. Therefore, it can be seen that the compressive behavior model for PVA-ECC can be also applied for PVA-ECC with CNTs.

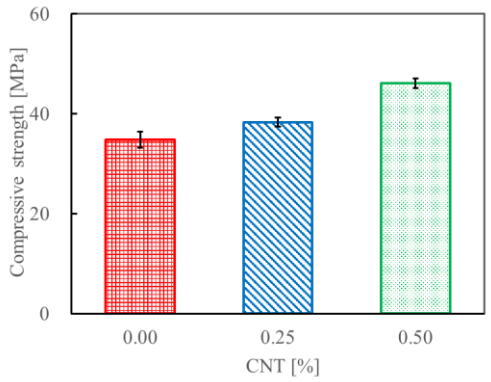

(a) Compressive strength

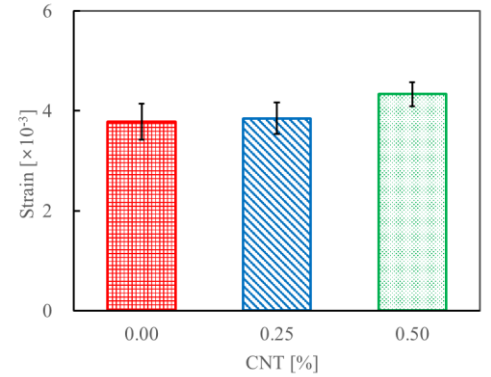

(b) Strain at the compressive strength

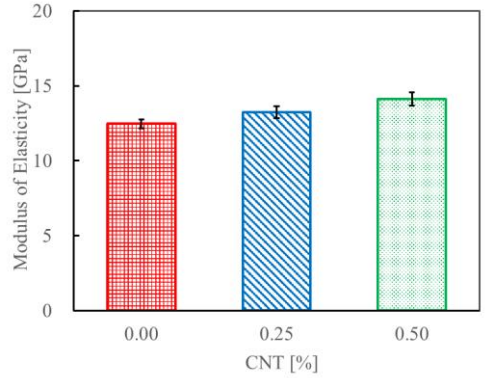

(c) Modulus of elasticity

Fig. 5 Compressive behavior graph of PVA-ECC with CNTs

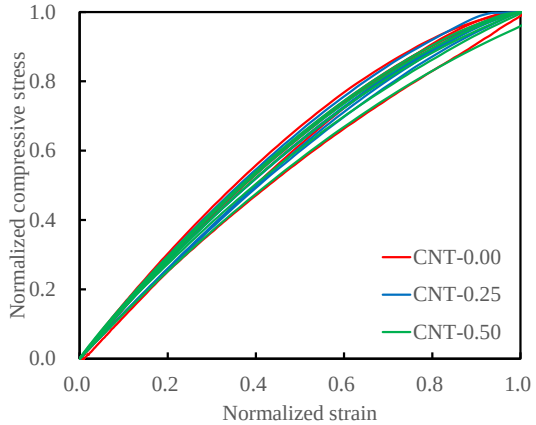

Fig. 6 Normalized compressive behavior

Table 4 Existing models for the compressive behavior

Reference	Model (for pre-peak)
Hognestad (1951)	$f_c = f_c'\left\{2\left(\frac{\varepsilon_c}{\varepsilon_{co}}\right) - \left(\frac{\varepsilon_c}{\varepsilon_{co}}\right)^2\right\}$
Popovics (1973)	$f_c = f_c'\left(\frac{\varepsilon_c}{\varepsilon_{co}}\right)\frac{n}{n-1+(\varepsilon_c/\varepsilon_{co})^k}$ $n = 0.80 + \frac{f_c'}{17}$
Lee *et al.*(2015)	$f_c = f_c'\left\{\frac{A(\varepsilon_c/\varepsilon_{co})}{A-1+(\varepsilon_c/\varepsilon_{co})^B}\right\}$ $A = B = \frac{1}{1-\left(\frac{f_c'}{\varepsilon_{co}E_c}\right)}$

Notation
f_c : compressive stress
f_c' : compressive strength
ε_c : compressive strain
ε_{co} : compressive strain at the compressive strength

4.3 Comparison with the existing models

To analyze the applicability of the existing models for the compressive behavior, the compressive stress-strain responses measured through the test were compared with the existing models. As the existing models, Hognestad (1951) and Popovics (1973) were considered, which were the most widely employed in structural analysis for normal and high strength concrete, respectively. In addition, as one of the most recently developed models for fiber reinforced concrete, Lee *et al.* (2015) was compared with the test results as well. Table 4 presents the summary of the three existing models for the pre-peak behavior under compression.

Fig. 7 compared the test results with the existing models according to the CNT mix ratio. As compared in the figure, Lee *et al.* (2015) proposed for fiber reinforced concrete showed the best agreement with the test results for PVA-ECC with or without CNTs. On the other hand, the other two models generally predicted that the curvature of the stress-strain response under compression was larger before reaching the compressive strength. As a result, the initial stiffness under compression was overestimated by the two models. This phenomenon can be explained by the effect of the coarse aggregate. When no coarse aggregate is mixed, the compressive behavior is closer to the linear response until the compressive strength is reached. Since PVA-ECC has coarse aggregate, it shows a behavior closer to that of the model proposed for fiber reinforce concrete with a less content of coarse aggregate.

4.4 SEM analysis

SEM image analysis was conducted to investigate the effect of CNTs in the microstructure of PVA-ECC. Noted that samples were taken near cracks in the cylindrical specimens after the compression test. SEM images were taken, mainly focused on two things; cement paste and PVA fibers.

Fig. 6 shows SEM images for microstructure of cement paste at the three levels of CNT mix ratio. Images were taken at resolutions of x1000 and x5000 considering the size of

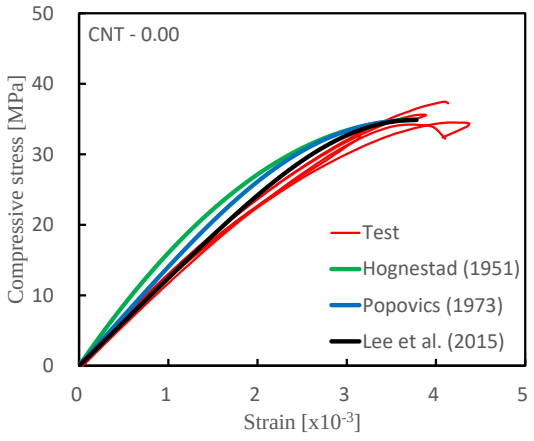

(a) 0.00 wt.% of CNT

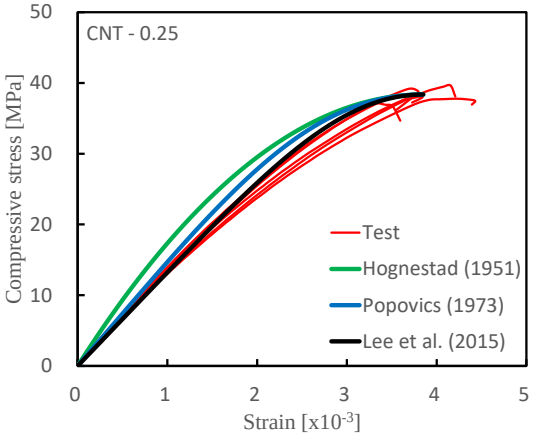

(b) 0.25 wt.% of CNT

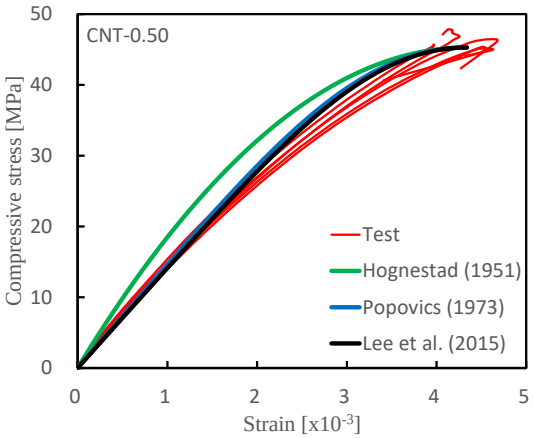

(c) 0.50 wt.% of CNT

Fig. 7 Comparison with the existing models

crystal and CNTs. As can be seen in the images with the x1000 resolution, lots of fly ash with spherical shape were easily found. It was also observed that a significant portion of the paste was occupied by amorphous hydrates in the form of dough. When the resolution was increased to x5000, CNTs in the form of solid lines, which were not easily seen at x1000 resolution, were easily found. It can be seen through the figure that CNTs were not only dispersed in the amorphous hydrates, but also adhered to the surface of the fly ash. This was quite different from PVA-ECC without CNTs; the surface of fly ash was left smooth. Therefore, it can be concluded that CNTs makes cement paste more compact, which is resulted with higher strength of concrete. In addition, since it looked that CNTs were well dispersed even with 0.50 wt.% of CNT mix ratio, the compressive behavior of PVA-ECC was improved with an addition of CNTs in this study.

Fig. 7 shows SEM images for PVA fibers. Images were taken at resolutions of x500 and x1000 considering the PVA fiber length and the CNT size. As shown in the figures, it was observed that the surface of the PVA fiber remained relatively clean when CNTs were not added. On the other hand, when CNTs were additionally mixed, amorphous hydrates with CNTs were found to stick on the surface of PVA fibers. In addition, it can be seen that more amorphous hydrates were attached to the surface of the PVA fiber as the CNT mix ratio increased. This trend means that the bond behavior of PVA fibers embedded in the cement paste is improved due to the incorporation of CNTs. That is, when the bond behavior of PVA fibers is improved, the splitting crack is more effectively controlled by PVA fibers after the compressive strength, so that a more ductile behavior can be expected for the post-peak under compression. In addition, it is estimated that the tensile behavior of PVA-ECC after cracking can be improved as well due to the bond behavior of PVA fibers improved with CNTs. Hence, due to the incorporation of CNTs, PVA-ECC can exhibit higher tensile stress after cracking as well as the cracking strength.

5. Conclusions

In this study, an experimental program has been conducted to investigate the effect of CNTs on the workability and the compressive behavior of PVA-ECC. SEM image analysis has been also conducted for the detailed investigation in the microstructure. The main results can be summarized as follows:

- As the CNTs mix ratio increased, the slump and slump flow significantly decreased. This is mainly due to high surface area of CNTs to hold water molecules. Especially, with 0.50 wt.% of CNTs, there was little slump. Therefore, it is required to properly determine the CNTs mix ratio with the consideration of workability.
- The compression test results showed that regardless of CNTs mix ratio, PVA-ECC exhibited almost linear stress-strain response until the compressive strength was reached since there was no coarse aggregate. Therefore, it is required to develop a constitutive model to represent the compressive behavior of PVA-ECC with or without CNTs.
- When the CNTs mix ratio increased up to 0.50 wt.%, the compressive strength increased by 32.1%, the strain corresponding to the compressive strength increased by 14.8%, and the modulus of elasticity increased by 12.8%. It can be, therefore, concluded that the compressive behavior of PVA-ECC can be improved as the CNTs mix ratio increases.
- Through the comparison on the normalized compressive behavior, it was investigated that the shape of the compressive behavior curve was little

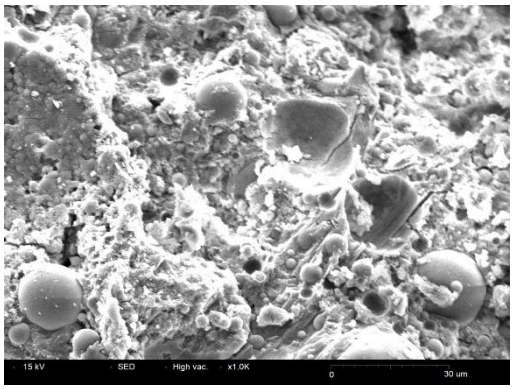
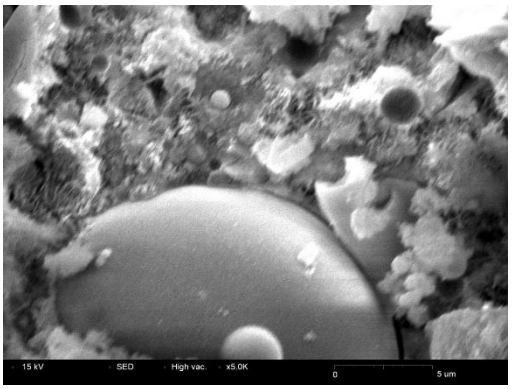

x1000 x5000

(a) 0.00 wt.% of CNT

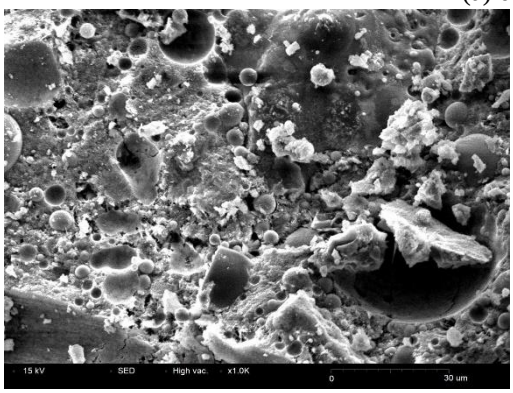
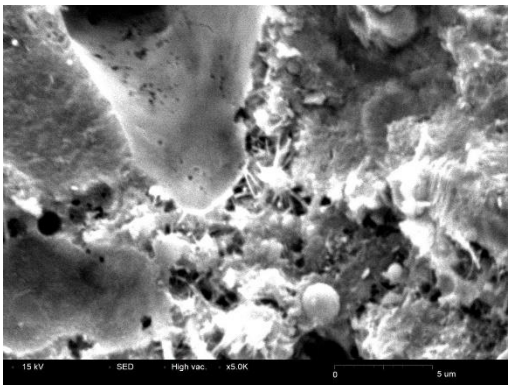

x1000 x5000

(b) 0.25 wt.% of CNT

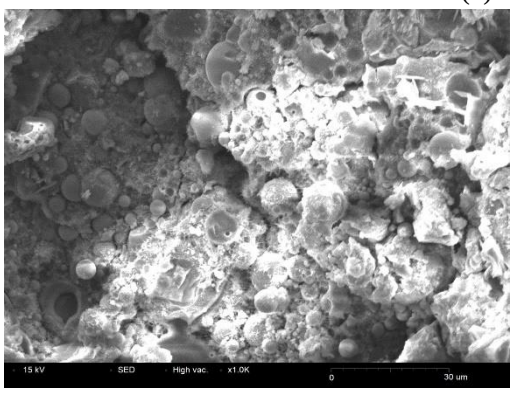
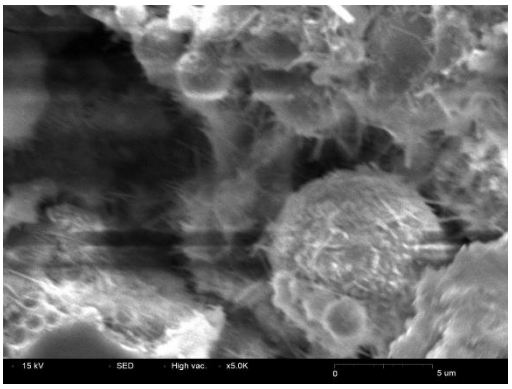

x1000 x5000

(c) 0.50 wt.% of CNT

Fig. 8 SEM images of ECC paste

affected by the CNTs. It can be seen, therefore, that CNTs has little effect on the shape of the compressive stress-strain response.

- From the SEM image analysis, it was observed that a large amount of CNTs were dispersed in amorphous hydrate or adsorbed on the surface of fly-ash. This indicated that the microstructure was denser due to the addition of CNTs. This leads to the result of increasing the strength of PVA-ECC.
- It was also observed that when CNT was not added, the surface of PVA fibers was relatively clean. On the other hands, a large amount of amorphous hydrate adhered to the surface of PVA fibers. Therefore, it can be inferred that the bond behavior of PVA fibers is considerably improved when CNTs are additionally mixed.

Acknowledgments

This work is supported by the Korea Agency for Infrastructure Technology Advancement (KAIA) grant funded by the Ministry of Land, Infrastructure and Transport (Grant 21NANO-B156177-02), and by Basic

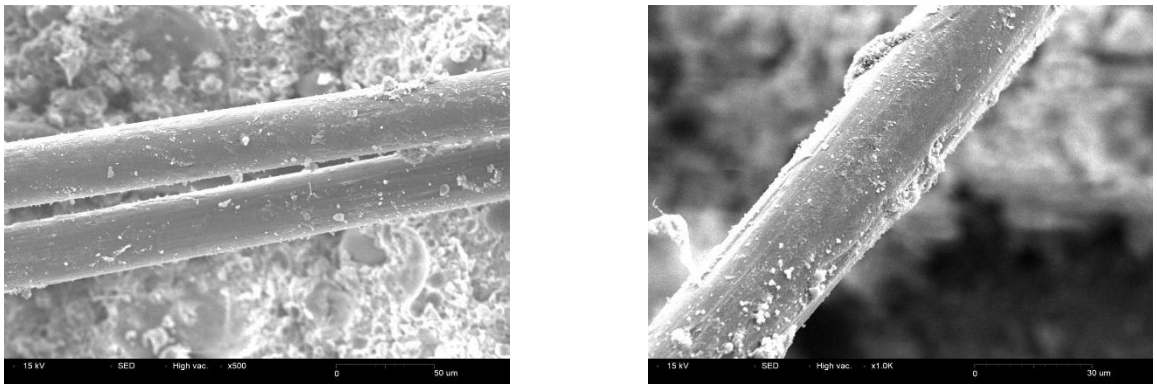

x500 x1000

(a) 0.00 wt.% of CNT

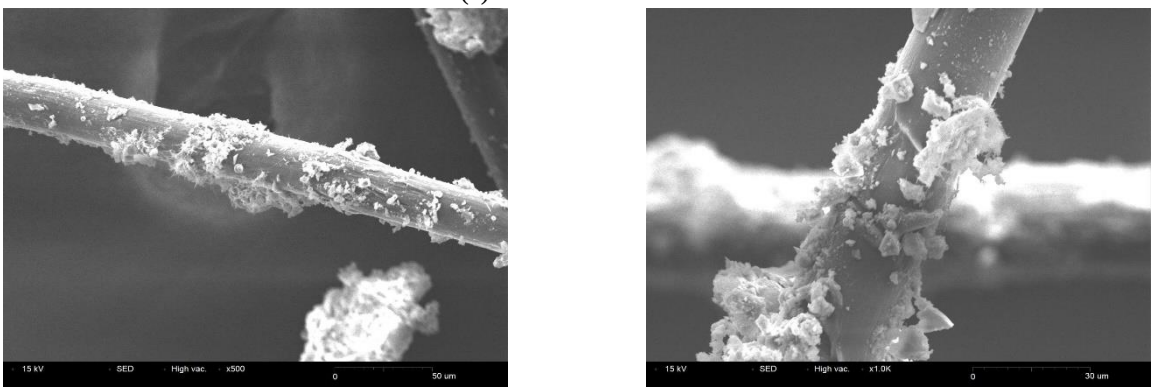

x500 x1000

(b) 0.25 wt.% of CNT

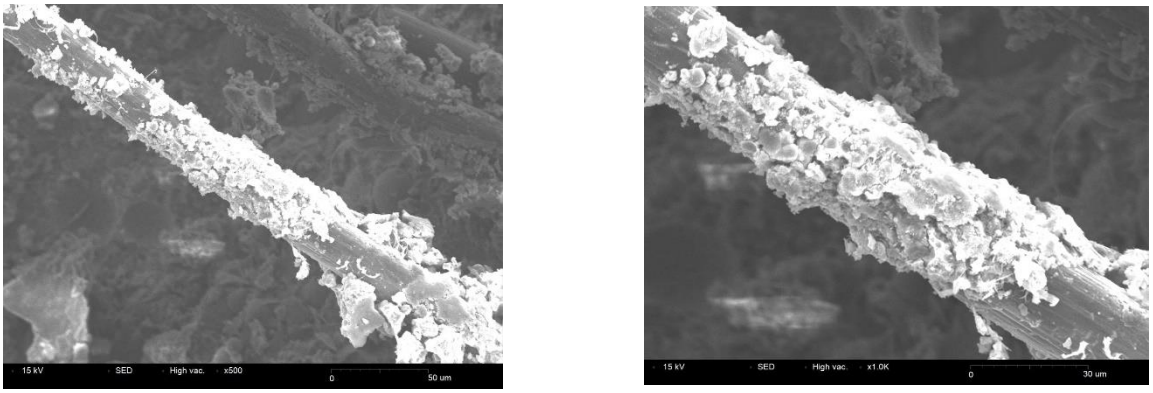

x500 x1000

(c) 0.50 wt.% of CNT

Fig. 9 SEM images of PVA fibers surface

Science Research Program through the National Research Foundation of Korea (NRF) funded by the Ministry of Education (NRF-2020R1I1A3073831).

References

ASTM C469-02 (2002), *Standard specification for testing method for static modulus of elasticity and poison's ratio of concrete in compression*. *2002 Annual Book of ASTM Standards,* American Society for Testing and Material, Philadelphia, Pennsylvania.

Bera, A.K. and Chakraborty, S. (2015), "Compaction and unconfined compressive strength of sand modified by class F fly ash", *Geomech. Eng.*, **9**(2), 261-273. https://doi.org/10.12989/gae.2015.9.2.261.

Bischoff, P.H. (2003), "Tension stiffening and cracking of steel fiber-reinforced concrete", *J. Mater. Civil Eng. - ASCE*, **15**(2), 174-182.

Camacho M. del C., Galao, O., Baeza F., Zornoza E. and Garcés, P. (2014), "Mechanical properties and durability of CNT cement composites", *Materials*, **7**(3), 1640-1651. https://doi.org/10.3390/ma7031640

Campillo, I., Dolado, J.S. and Porro, A. (2004), "High-performance nanostructured materials for construction", *Special*

Publication-Royal Society of Chemistry, **292**, 215-226. https://doi.org/10.1039/9781847551528-00215.

Caratelli, A., Meda, A., Rinaldi, Z. and Romualdi, P. (2011), "Structural behaviour of precast tunnel segments in fiber reinforced concrete", *Tunn. Undergr. Sp. Tech.*, **26**(2), 284-291. https://doi.org/10.1016/j.tust.2010.10.003.

Chen, G.H., Zou, J.F. and Qian, Z.H. (2019), "An improved collapse analysis mechanism for the face stability of shield tunnel in layered soils", *Geomech. Eng.*, **17**(1), 97-107. https://doi.org/10.12989/gae.2019.17.1.097.

Chen, S.J., Collins, F.G., MacLeod, A.J.N., Pan, Z., Duan, W.H., and Wang, C.M. (2011), "Carbon nanotube–cement composites: A retrospect", *The IES J. part a: Civil Struct. Eng.*, **4**(4), 254-265. https://doi.org/10.1080/19373260.2011.615474.

Collins, F., Lambert, J. and Duan, W.H. (2012), "The influences of admixtures on the dispersion, workability, and strength of carbon nanotube–OPC paste mixtures", *Cement Concrete Compos.*, **34**(2), 201-207. https://doi.org/10.1016/j.cemconcomp.2011.09.013.

Deluce, J.R., Lee, S.C. and Vecchio, F.J. (2014), "Crack model for steel fiber-reinforced concrete members containing conventional reinforcement", *ACI Struct. J.*, **111**(1), 93-102.

Demirboğa, R. (2003), "Influence of mineral admixtures on thermal conductivity and compressive strength of mortar", *Energ. Build.*, **35**(2), 189-192. https://doi.org/10.1016/S0378-7788(02)00052-X

Gettu, R., Barragán, B., García, T., Ramos, G., Fernández, C. and Oliver, R. (2004), "Steel fiber reinforced concrete for the Barcelona metro line 9 tunnel lining", *Proceedings of the 6th RILEM Symposium on FRC,* Varenna, Italy, RILEM PRO.

Hawreen, A., Bogas, J.A. and Dias, A.P.S. (2018), "On the mechanical and shrinkage behavior of cement mortars reinforced with carbon nanotubes", *Constr. Build. Mater.*, **168**, 459-470. https://doi.org/10.1016/j.conbuildmat.2018.02.146.

Hognestad E. (1951), "A study of combined bending and axial load in reinforced concrete members", Bulletin Series No. 399, Engineering Experiment Station, Urbana, USA, University of Illinois.

Iijima, S. (1991), "Helical microtubules of graphitic carbon", *Nature*, **354**(6348), 56-58. https://doi.org/10.1038/354056a0.

Isfahani, F.T., Li, W. and Redaelli, E. (2016), "Dispersion of multi-walled carbon nanotubes and its effects on the properties of cement composites", *Cement Concrete Compos.*, **74**, 154-163. https://doi.org/10.1016/j.cemconcomp.2016.09.007.

Karabash, Z. and Cabalar, A.F. (2015), "Effect of tire crumb and cement addition on triaxial shear behavior of sandy soils", *Geomech. Eng.*, **8**(1), 1-15. http://dx.doi.org/10.12989/gae.2015.8.1.001.

Kim, J.K., Kim, J.S., Ha, G.J. and Kim, Y.Y. (2007), "Tensile and fiber dispersion performance of ECC (engineered cementitious composites) produced with ground granulated blast furnace slag", *Cement Concrete Res.*, **37**(7), 1096-1105. https://doi.org/10.1016/j.cemconres.2007.04.006.

Lee, D.K., Lee, K.C., Lee, C.D. and Shin, K.J. (2019), "Study on ECC tensile behavior due to constrained drying shrinkage", *J. Korean Recycled Constr. Resour. Inst.*, 7(4), 367-374. https://doi.org/10.14190/JRCR.2019.7.4.367.

Lee, S.C., Cho, J.Y. and Vecchio, F.J. (2013a), "Tension-stiffening model for steel fiber-reinforced concrete containing conventional reinforcement", *ACI Struct. J.*, **110**(4), 639-648.

Lee, S.C., Cho, J.Y. and Vecchio, F.J. (2013b), "Simplified diverse embedment model for steel fiber-reinforced concrete elements in tension", *ACI Mater. J.*, **110**(4), 403-412.

Lee, S.C., Kim, J.H., Cho, J.Y. and Shin, K.J. (2010), "Tension stiffening of reinforced high performance fiber reinforced cementitious composites (HPFRCC)", *J. Korea Concrete Institute*, **22**(6), 859-866. https://doi.org/10.4334/jkci.2010.22.6.859.

Lee, S.C., Oh, J.H. and Cho, J.Y. (2015), "Compressive behavior of fiber-reinforced concrete with end-hooked steel fibers", *Materials*, **8**(4), 1442-1458. https://doi.org/10.3390/ma8041442.

Li, G.Y., Wang, P.M. and Zhao, X. (2005), "Mechanical behavior and microstructure of cement composites incorporating surface-treated multi-walled carbon nanotubes", *Carbon*, **43**(6), 1239-1245. https://doi.org/10.1016/j.carbon.2004.12.017.

Li, G.Y., Wang, P.M. and Zhao, X. (2007), "Pressure-sensitive properties and microstructure of carbon nanotube reinforced cement composites", *Cement Concrete Compos.*, **29**(5), 377-382. https://doi.org/10.1016/j.cemconcomp.2006.12.011.

Lim, T.Y., Paramasivam, P. and Lee, S.L. (1987), "Analytical model for tensile behavior of steel-fiber concrete", *ACI Mater. J.*, **84**(4), 286-298.

Magalhães, M. da S., Toledo Filho, R.D. and Fairbairn, E. de M.R. (2015), "Thermal stability of PVA fiber strain hardening cement-based composites", *Constr. Build. Mater.*, **94**, 437-447. https://doi.org/10.1016/j.conbuildmat.2015.07.039.

Marti, P., Pfyl, T., Sigrist, V. and Ulaga, T. (1999), "Harmonized test procedures for steel fiber-reinforced concrete", *ACI Mater. J.*, **96**(6), 676-686.

Meda, A., Rinaldi, Z., Spagnuolo, S., De Rivaz, B. and Giamundo, N. (2019), "Hybrid precast tunnel segments in fiber reinforced concrete with glass fiber reinforced bars", *Tunn. Undergr. Sp. Tech.*, **86**, 100-112. https://doi.org/10.1016/j.tust.2019.01.016.

Mohsen, M.O., Al Ansari, M.S., Taha, R., Al Nuaimi, N. and Taqa, A.A. (2019), "Carbon nanotube effect on the ductility, flexural strength, and permeability of concrete", *J. Nanomater.*, **2019**, 1-11. https://doi.org/10.1155/2019/6490984.

Musso, S., Tulliani, J.M., Ferro, G. and Tagliaferro, A. (2009), "Influence of carbon nanotubes structure on the mechanical behavior of cement composites", *Compos. Sci. Technol.*, **69**(11-12), 1985-1990. https://doi.org/10.1016/j.compscitech.2009.05.002.

Na, C. and Kwak, H.G. (2011), "A numerical tension-stiffening model for ultra high strength fiber-reinforced concrete beams", *Comput. Concrete*, **8**(1), 1-22.

Nochaiya, T., Tolkidtikul, P., Singjai, P. and Chaipanich, A. (2008), "Microstructure and characterizations of portland-carbon nanotubes pastes", *Adv. Mater. Res.*, **55**, 549-552. https://doi.org/10.4028/www.scientific.net/amr.55-57.549.

Park, S.H., Sim, Y., Lee, W., Cho, S.K., Lee, D., Lee, S.C. and Yoo, S.W. (2021), "Material behavior of PVA cementitious composites with CNTs according to the mixing order", *Proceedings of KSCE convention.*

Popovices, S. (1973), "A numerical Approach to the complete stress-strain curve of concrete", *Cement Concrete Res.*, **3**(5), 583-599.

Rhee, I. and Roh, Y.-S. (2013), "Properties of normal-strength concrete and mortar with multi-walled carbon nanotubes", *Mag. Concrete Res.*, **65**(16), 951-961. https://doi.org/10.1680/macr.12.00212.

Rousakis, T.C., Kouravelou, K.B. and Karachalios, T.K. (2014), "Effects of carbon nanotube enrichment of epoxy resins on hybrid FRP–FR confinement of concrete", *Compos. Part B: Eng.*, **57**, 210-218. https://doi.org/10.1016/j.compositesb.2013.09.044.

Ruoff, R.S. and Lorents, D.C. (1995), "Mechanical and thermal properties of carbon nanotubes", *Carbon*, **33**(7), 925-930. https://doi.org/10.1016/0008-6223(95)00021-5.

Shao, H., Chen, B., Li, B., Tang, S. and Li, Z. (2017), "Influence of dispersants on the properties of CNTs reinforced cement-based materials", *Constr. Build. Mater.*, **131**, 186-194. https://doi.org/10.1016/j.conbuildmat.2016.11.053.

Shi, B. and Kong, X. (2016), "Study of the diseases of shield

tunnels and its reasons", *Geo-China*, **2016**, 40-45. https://doi.org/10.1061/9780784480038.006

Shin, K.J., Kim, J.H., Cho, J.Y. and Lee, S.C. (2011), "Flexural behavior of high performance fiber reinforced cementitious composites (HPFRCC) beam with a reinforcing bar", *J. Korea Concrete Inst.*, **23**(2), 169-176. https://doi.org/10.4334/jkci.2011.23.2.169.

Shin, K.J., Jang, K.H., Choi, Y.C. and Lee, S.C. (2015), "Flexural behavior of HPFRCC members with inhomogeneous material properties", *Materials*, **8**(4), 1934-1950. https://doi.org/10.3390/ma8041934.

Shooshpasha, I. and Shirvani, R.A. (2015), "Effect of cement stabilization on geotechnical properties of sandy soils", *Geomech. Eng.*, **8**(1), 17-31. http://doi.org/10.12989/gae.2015.8.1.017.

Silvestro, L. and Jean Paul Gleize, P. (2020), "Effect of carbon nanotubes on compressive, flexural and tensile strengths of Portland cement-based materials: A systematic literature review", *Constr. Build. Mater.*, **264**, 120237. https://doi.org/10.1016/j.conbuildmat.2020.120237.

Taha, M.R., Alsharef, J.M., Khan, T.A., Aziz, M. and Gaber, M. (2018), "Compressive and tensile strength enhancement of soft soils using nanocarbons", *Geomech. Eng.*, **16**(5), 559-567. https://doi.org/10.12989/gae.2018.16.5.559.

Tanaka, K., Sato, T., Yamabe, T., Okahara, K., Uchida, K., Yumura, M. and Ikazaki, F. (1994), "Electronic properties of carbon nanotube", *Chem. Phys. Lett.*, **223**(1-2), 65-68. https://doi.org/10.1016/0009-2614(94)00421-8.

Voo, J.Y.L. and Foster, S.J. (2003), "Variable engagement model for fibre reinforced concrete in tension", Uniciv Report No. R-420, University of New South Wales, School of Civil and Environmental Engineering, 86.

Wang, Z., Yu, J., Li, G., Zhang, M. and Leung, C.K. (2019), "Corrosion behavior of steel rebar embedded in hybrid CNTs-OH/polyvinyl alcohol modified concrete under accelerated chloride attack", *Cement Concrete Compos.*, **100**, 120-129. https://doi.org/10.1016/j.cemconcomp.2019.02.013.

Yan, Z., Zhu, H. and Ju, J.W. (2013), "Behavior of reinforced concrete and steel fiber reinforced concrete shield TBM tunnel linings exposed to high temperatures", *Constr. Build. Mater.*, **38**, 610-618. https://doi.org/10.1016/j.conbuildmat.2012.09.019.

Yilmaz, Y., Cetin, B. and Kahnemouei, V.B. (2017), "Compressive strength characteristics of cement treated sand prepared by static compaction method", *Geomech. Eng.*, **12**(6), 935-948. https://doi.org/10.12989/gae.2017.12.6.935.

Yoo, D.Y., Kim, S. and Lee, S.H. (2018), "Self-sensing capability of ultra-high-performance concrete containing steel fibers and carbon nanotubes under tension", *Sensor. Actuat. A: Phys.*, **276**, 125-136. https://doi.org/10.1016/j.sna.2018.04.009

You, I., Yoo, D.Y., Kim, S., Kim, M.J. and Zi, G. (2017), "Electrical and self-sensing properties of ultra-high-performance fiber-reinforced concrete with carbon nanotubes", *Sensors*, **17**(11), 2481. https://doi.org/10.3390/s17112481.

Xu, G., He, C., Lu, D. and Wang, S. (2019), "The influence of longitudinal crack on mechanical behavior of shield tunnel lining in soft-hard composite strata", *Thin-Wall. Struct.*, **144**, 106282. https://doi.org/10.1016/j.tws.2019.106282.

Xue, Y., Li, X., Li, G., Qiu, D., Gong, H. and Kong, F. (2020), "An analytical model for assessing soft rock tunnel collapse risk and its engineering application", *Geomech. Eng.*, **23**(5), 441-454. https://doi.org/10.12989/gae.2020.23.5.441.